Engineering Structures 109 (2016) 16–25

Contents lists available at ScienceDirect

Engineering Structures

journal homepage: www.elsevier.com/locate/engstruct

# An experimental investigation of shear-transfer strength of normal and high strength self compacting concrete

K.N. Rahal *, A.L. Khaleefi, A. Al-Sanee

*Civil Engineering Department, Kuwait University, P.O. Box 5969, Safat 13060, Kuwait*

ARTICLE INFO

*Article history:*
Received 28 October 2014
Revised 19 November 2015
Accepted 23 November 2015

*Keywords:*
Aggregate interlock
Codes
Dowel action
Self-compacting concrete
Shear
Deformation
Strength

ABSTRACT

Fifteen non-precracked pushoff specimens were tested to investigate the shear-transfer behavior of normal strength and high strength self-compacting concrete (SCC). The reported results include the cracking stresses, the yielding stresses, the ultimate strengths and the post-ultimate residual strengths. It is shown that the specimens resisted significant post-ultimate residual strengths and shear slip values reaching 20 mm. It is also shown that increasing the compressive strength of the concrete significantly increased the ultimate shear strength but had a limited effect on the cracking and the residual strengths. The calculations of four existing models are compared with the observed ultimate strengths, and the calculated strengths are generally conservative. The AASHTO shear-friction and the SMCS models provide the best correlation with the experimental results. The possibility of using existing models to calculate the residual strength is also investigated. The shear transfer planes are assumed to be precracked, and the roughness conditions are selected based on the expected path of the cracks relative to the coarse aggregates. Eurocode 2 (EC2) provides the best correlations while the ACI calculations are generally conservative. The residual strengths from 30 pushoff specimens are analyzed. A shear friction equation with a coefficient of cohesion equal to zero, a coefficient of friction equal to 1.0, and an upper limit on the stress equal to 5.5 MPa is found to provide adequate calculation of the residual strength of non-precracked pushoff specimens.



## 1. Introduction

Shear-transfer models which are based on the shear-friction theory (e.g. [1–3]) are semi-empirical models that have been calibrated using experimental data obtained mainly from pushoff specimens (e.g. [4–7]). They can be used to design the transfer of shear across a cold joint or across an existing crack. The transfer can also be across a critical plane not previously cracked, such as the bearing region of a simple girder or the interface between a corbel and the supporting column. See Fig. 1.

Experimental data used in the calibration of these semi-empirical models is available from three main types of pushoff specimens which differ mainly by the conditions at the shear transfer plane: (1) specimens that were precracked, (2) specimens that were not precracked, and (3) specimens that were cast at two different times (with a cold joint). Fig. 2 plots a summary of a survey of the number of available test results from conventional pushoff specimens (with conventional reinforcing bars, and with no applied flexure or axial stresses perpendicular along shear plane) [4–19]. The plot gives separate counts for specimens with normal strength concrete (NSC) (with compressive strength less than 50 MPa) and for relatively higher strength concrete (with strength larger than 50 MPa). The figure shows that there is a limited amount of data from high strength concrete (HSC) uncracked specimens. Recent studies also showed that existing analytical models focus largely on the cases of precracked interfaces and cold joints [20,21]. This research aimed at providing more data on non-precracked HSC specimens.

On the other hand, it has been observed by Mattock et al. [14] that after reaching the ultimate shear strength, non-precracked pushoff specimens resisted a residual strength which was similar to the strength of the precracked specimens. The tests by Kahn and Mitchell [4] and the Finite Element analysis by Xu et al. [22] confirmed this observation. In spite of its practical importance, this residual strength has not been typically reported separately from the ultimate strength. This research aimed at adding to the limited available tests results which differentiate between the ultimate and the residual strengths.

The stresses at which shear cracks first develop are of importance. For example, these values can be used to establish a benchmark for the selection of the minimum amount of clamping

* Corresponding author. Tel.: +965 2481 7240; fax: +965 2481 7524.
*E-mail address:* khaldoun.rahal@ku.edu.kw (K.N. Rahal).

http://dx.doi.org/10.1016/j.engstruct.2015.11.015
0141-0296/

**Nomenclature**

| | |
|---|---|
| $c$ | coefficient related to cohesion |
| $f'_c$ | specified compressive strength of concrete (cylinder) |
| $f_{cd}$ | design compressive strength of concrete (EC2) |
| $f_{ck}$ | characteristic compressive strength of concrete at 28 days (EC2) |
| $f_{ctd}$ | design tensile strength of concrete (EC2) |
| $f_{cu}$ | compressive strength of 150 mm concrete cube |
| $f_{cy}$ | compressive strength of standard concrete cylinder |
| $f_y$ | yield strength of reinforcement |
| $f_{yL}$ | yield strength of longitudinal reinforcement |
| $f_{yv}$ | yield strength of clamping reinforcement |
| $v_{cr}$ | cracking shearing stress |
| $v_{cr\text{-}A}$ | cracking shearing stress calculated using ACI equation |
| $v_r$ | observed post-ultimate residual shearing strength |
| $v_{r\text{-}AASHTO}$ | residual shearing strength (AASHTO specifications) |
| $v_{r\text{-}ACI}$ | residual shearing strength (ACI code) |
| $v_{r\text{-}EC2}$ | residual shearing strength (EC2 code) |
| $v_{r\text{-}Mat}$ | residual shearing strength (Mattock model) |
| $v_u$ | observed ultimate shearing strength |
| $v_{u\text{-}AASHTO}$ | nominal shearing strength (AASHTO specifications) |
| $v_{u\text{-}ACI}$ | nominal shearing strength (ACI code) |
| $v_{u\text{-}Mat}$ | nominal shearing strength (Mattock model) |
| $v_{u\text{-}SMCS}$ | nominal shearing strength (SMCS model) |
| $v_y$ | observed yielding shearing stress |
| $\eta$ | strength reduction factor (EC2 code) |
| $\rho_L$ | ratio of longitudinal reinforcement (parallel to shear transfer plane) |
| $\rho_v$ | ratio of clamping reinforcement perpendicular to shear transfer plane |
| $\mu$ | coefficient of friction in shear friction models |
| $\omega_L$ | reinforcement index in longitudinal direction (SMCS model) |
| $\omega_v$ | reinforcement index in transverse direction (SMCS model) |

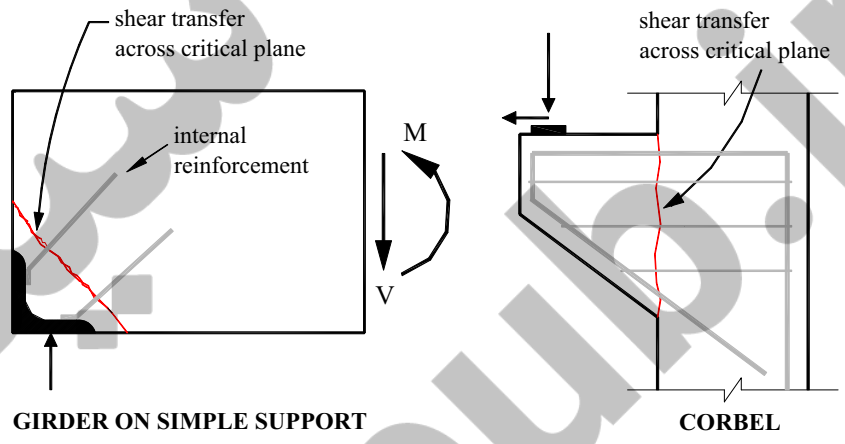


**Fig. 1.** Transfer of shear across critical planes not previously cracked.

reinforcement. The cracking shearing stresses are not typically reported in pushoff tests. This research aimed at providing information on the cracking shearing stresses.

Hence, this paper reports the results of an experimental program which aimed at gaining a better understanding of the behavior of non-precracked HSC pushoff specimens. Since the use of self-compacting concrete (SCC) is on the rise around the globe, the concrete used was made with SCC properties. The results from 15 specimens are reported. Twelve of the specimens were SCC (six NSC and six HSC specimens), and three specimens were normal strength conventional concrete. The three conventional concrete specimens are control specimens. The experimental behavior and strengths are given, including a detailed account of the cracking, yield, ultimate and residual stresses.

In addition to reporting the experimental results, this paper also compares between the observed ultimate strengths and the calculations of the shear-transfer models of the ACI code [1], the AASHTO LRFD Specifications [2], the Mattock's tri-linear empirical model [3], and the simplified model for combined stress-resultants (SMCS) model [23]. This paper also investigates the possibility of

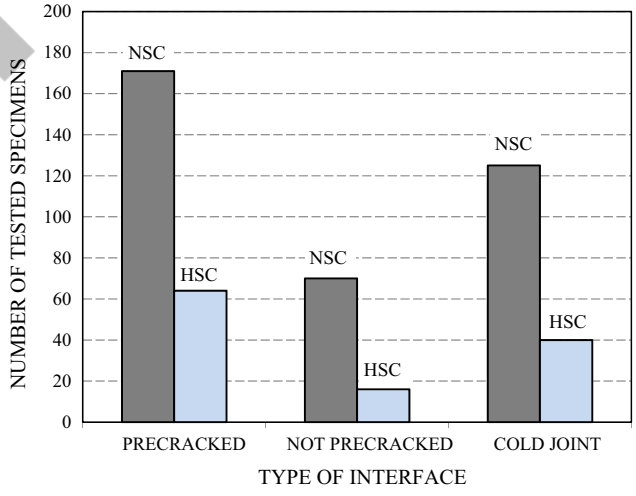


**Fig. 2.** Number of reported pushoff tests in literature.

**Table 1**
Details of the test specimens and summary of experimental results.

| Series | Specimen | Clamp. steel | $\rho_t f_{yv}$ (MPa) | $f_{cu}$ (MPa) | $f_{cy}$ (MPa) | $v_{cr}$ (MPa) | $v_y$ (MPa) | $v_u$ (MPa) | $v_r$ (MPa) | $\frac{v_y}{v_u}$ | $\frac{v_r}{v_u}$ |
|---|---|---|---|---|---|---|---|---|---|---|---|
| SCC35 | 35-2T6-SCC | 2$\phi$6 | 0.93 | 43.7 | – | 4.4 | 5.5 | 6.1 | 1.6 | 0.90 | 0.26 |
| | 35-2T8-SCC | 2$\phi$8 | 2.63 | | | 5.0 | 7.0[a] | 7.33 | 3.3 | 0.95 | 0.45 |
| | 35-3T8-SCC | 3$\phi$8 | 3.94 | | | 4.9 | 7.6 | 7.70 | 5.6 | 0.99 | 0.73 |
| | 35-3T8-SCCr[b] | 3$\phi$8 | 3.94 | | | 5.2 | 8.5 | 8.79 | 4.2 | 0.97 | 0.48 |
| | 35-4T8-SCC | 4$\phi$8 | 5.25 | | | 6.5 | 9.0[a] | 9.70 | 5.3 | 0.93 | 0.55 |
| | 35-6T8-SCC | 6$\phi$8 | 7.88 | | | 6.6 | 10.8[a] | 11.1 | 5.5 | 0.97 | 0.50 |
| SCC70 | 70-2T6-SCC | 2$\phi$6 | 0.93 | 79.2 | 81.2 | 3.9 | 6.4 | 8.69 | 2.0 | 0.74 | 0.23 |
| | 70-2T8-SCC | 2$\phi$8 | 2.63 | | | 6.8 | 9.0 | 11.50 | 4.6 | 0.78 | 0.40 |
| | 70-3T8-SCC | 3$\phi$8 | 3.94 | | | 6.0 | 11.7 | 12.57 | 4.6 | 0.93 | 0.37 |
| | 70-3T8-SCCr[b] | 3$\phi$8 | 3.94 | | | 5.6 | 12.2 | 12.3 | 4.9 | 0.99 | 0.40 |
| | 70-4T8-SCC | 4$\phi$8 | 5.25 | | | 5.3 | 12.7 | 12.77 | 6.1 | 0.99 | 0.48 |
| | 70-6T8-SCC | 6$\phi$8 | 7.88 | | | 6.8 | 15.8 | 15.85 | 5.6 | 1.00 | 0.35 |
| N35 | 35-2T6-0 | 2$\phi$6 | 0.93 | 43.4 | 41.8 | 5.44 | 5.25[a] | 5.55 | 2.0 | 0.95 | 0.36 |
| | 35-2T8-0 | 2$\phi$8 | 2.63 | | | 6.72 | 7.55 | 7.94 | 3.9 | 0.95 | 0.49 |
| | 35-3T8-0 | 3$\phi$8 | 3.94 | | | 5.44 | 7.75 | 8.68 | 4.9 | 0.89 | 0.56 |
| | | | | | | Average | | | | 0.93 | 0.44 |
| | | | | | | Coefficient of variation (%) | | | | 8.2 | 28.2 |

[a] Yield was recorded slightly after ultimate stress was reached.
[b] Longitudinal reinforcement 8$\phi$12.

using the EC2 [24], ACI and AASHTO code equations and Mattock's model to calculate the residual strength.

## 2. Experimental program

Fifteen pushoff specimens were cast and tested to failure. The specimens were cast in three different groups: the normal strength SCC group (SCC35), the high strength SCC group (SCC70), and the normal strength conventional concrete group (N35). Table 1 provides some of the details of the three groups. Specimens of the same group differed by the number and size of the clamping reinforcement provided, except for two specimens of each of the SCC series which contained the same amount of clamping reinforcement as two companion specimens but different amounts of longitudinal (vertical) reinforcement. The target compressive strength in the three groups was 35 MPa in the SCC35 and the N35 series, and 70 MPa in the SCC70 series.

### 2.1. Pushoff specimens

Fig. 3 shows the details of the specimens. The capacity of the clamping steel ($\rho_t f_{yv}$) ranged from 0.93 to 7.9 MPa. The slip deformation across the transfer plane was measured. The strain in this steel was also measured using a strain gauge which was attached to a central clamp at the intersection of one of the legs with the shear-transfer plane as shown in Fig. 3.

### 2.2. Concrete materials and mixes

Table 2 summarizes the mix proportions of the concrete. Type I cement conforming to the requirements of ASTM C 150 and tap water were used in all specimens. Silica fume conforming to the requirements of ASTM C 1240 was used in the SCC70 series. The coarse aggregates were crushed limestone while the fine aggregates were sand. All aggregates were used in their air-dry conditions.

High-range water reducing (HRWR) admixtures conforming to ASTM C494 types G and F and ASTM C1017 types 1 and 2 were used in all mixes. Those used in the two SCC mixes were polycarboxylate ether-based, while those used in series N35 were naphthalene based admixtures. The amount of water added to the mixes was adjusted to compensate for the moisture conditions of the aggregates.

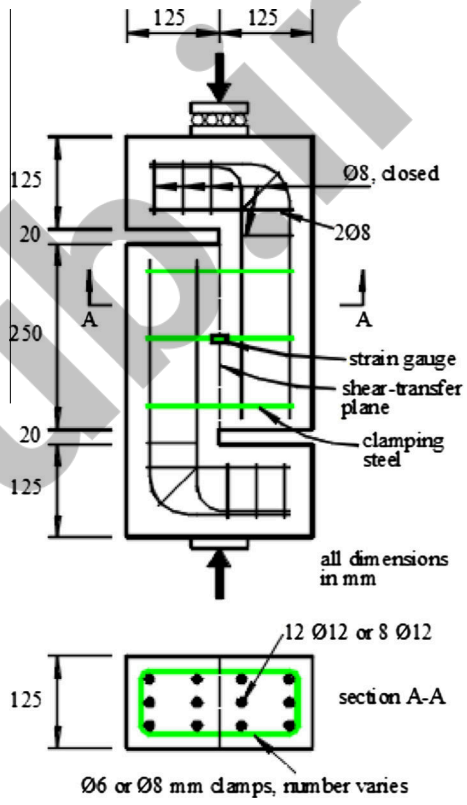


**Fig. 3.** Dimensions and reinforcement of pushoff specimens.

Slump flow tests were conducted on the SCC mixes in accordance with ASTM C1161. The slump flow values were 670 mm for the SCC35 concrete and 620 mm for the SCC70. The slump of the concrete of series N35 was 140 mm. The concrete was also visually inspected and no signs of segregation were observed.

### 2.3. Reinforcing steel

The tensile strength of the reinforcing steel bars was tested in accordance with the ASTM A370-07 standard. The results are summarized in Table 3

**Table 2**
Mix proportions.

| Series | Cement (kg/m$^3$) | Silica (kg/m$^3$) | Coarse Aggregates (kg/m$^3$) | | | | Natural sand (kg/m$^3$) | Water (kg/m$^3$) | HRWR ($\ell$/m$^3$) |
|---|---|---|---|---|---|---|---|---|---|
| | | | 20-mm | 12.5-mm | 10-mm | 3-mm | | | |
| SCC35 | 489 | – | 556 | – | 402 | – | 858 | 190 | 12.5 |
| SCC70 | 509 | 54.5 | – | – | 808 | 462 | 548 | 165 | 15.7 |
| N35 | 410 | – | 260 | 340 | 500 | – | 705 | 185 | 6.0 |

**Table 3**
Properties of reinforcing steel bars.

| Nominal diameter (mm) | $f_y$ (MPa) | $f_u$ (MPa) |
|---|---|---|
| 6 | 258 | 326 |
| 8 | 408 | 733 |
| 12 | 453 | 770 |

### 2.4. Casting and testing

All pushoff specimens of each of a specific series were cast from the same batch. In addition, standard size cylinders and 150-mm cubes were cast from the concrete of each of the mixes. Metal molds were used to cast all the specimens. The conventional concrete was compacted using an electric vibrator.

After casting, all the concrete was covered with wet burlap and plastic sheets. Twenty four hours later, the specimens were stripped from the molds and were placed in a water tank in the lab to cure. The average strength of the concrete cubes $f_{cu}$ and the concrete cylinders $f_{cy}$ on the day of testing are given in Table 1.

The specimens were placed vertically and loaded concentrically as shown in Fig. 3. The loading was monotonic, and the rate of deformation applied by the machine was 1 mm/min for all the specimens. Clamping steel strains and shear deformation (slip) across the transfer plane were measured at very close intervals. Special attention was also given to visually detecting the occurrence of the surface cracks as soon as they developed.

## 3. Experimental results

The experimental results are summarized in Table 1. The following sections discuss the main observations in more details

### 3.1. General behavior of the pushoff specimens

Fig. 4 shows the shear stress versus the shear deformation across the transfer planes in two of the SCC specimens. Both specimens were reinforced with three 8-mm clamps, but one was from the NSC series SCC35 and the other was from the HSC series SCC70. Fig. 5 shows the test region of the HSC specimen at three different stages of the loading.

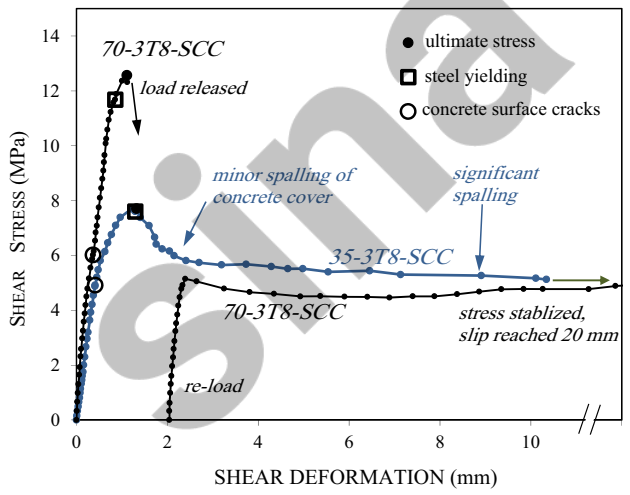


**Fig. 4.** Observed response of normal and high strength SCC specimens.

The response of 35-3T8-SCC was characterized by three distinct zones. In the first zone and as the load increased, surface concrete cracks developed along the shear-transfer plane (at a shearing stress referred to as $v_{cr}$). Further loading caused additional cracking and caused the strains in the clamps to reach the onset of yield (at a shearing stress referred to as $v_y$). Yielding was soon followed by reaching the ultimate strength ($v_u$). The behavior was relatively linear in the ascending zone of the response, with softening becoming obvious only as the stress approached $v_y$. After reaching the ultimate stress, the resistance decreased significantly. The end of the descending zone was characterized by the development of limited spalling on the surface concrete near the shear transfer plane. The application of further deformation was achieved at a relatively constant stress. Fig. 4 shows that the specimen was capable of sustaining a significant amount of shear deformation at a relatively constant shear stress in the third zone of the response. This stress is referred to as the residual strength $v_r$, and was taken as the average stress which was measured for slip values in the range between 10 mm and 20 mm. The tests were stopped when the side openings in the specimens nearly closed up, which corresponds to a slip deformation of about 20 mm.

Unlike the observation in the normal strength concrete specimen, the reduction in the resistance of 70-3T8-SCC after ultimate was very sudden. It caused the control of the testing machine to disengage and shut off. Fig. 5(a) shows the conditions of this specimen after the release of the load. Limited spalling of the concrete cover was observed. The application of the loading was resumed as shown in Fig. 4, and the resistance was significantly lower than the previously attained ultimate stress. In fact, the reload resistance was the residual strength. Fig. 5(b) shows the significant spalling of the concrete cover when the shear deformation reached about 6 mm. Fig. 5(c) shows the final condition of the specimen after release of load. Damage affected not only the cover concrete but also a part of the core concrete within the clamping steel. The deformation in the clamping bars due to dowel effect is evident. Fig. 4 shows that the residual strength of the HSC specimen is not significantly different from that of the NSC specimen with the same clamping steel.

### 3.2. Cracking stresses

The cracking shear stresses ($v_{cr}$) which caused the first development of surface cracks are reported in Table 1. These cracks appeared along the shear transfer plane. They were typically vertical, but in some cases they were inclined. In general, these cracks were not accompanied by a significant softening in the shear stress-deformation response as shown in Fig. 4.

Fig. 6 plots the cracking shearing stresses versus the amount of clamping reinforcement ($\rho_t f_{yv}$) for the three series of specimens. In the SCC specimens of the same group which contained similar amounts of clamps, average values are plotted. A very large scatter in the results is observed. It is shown that in general, the

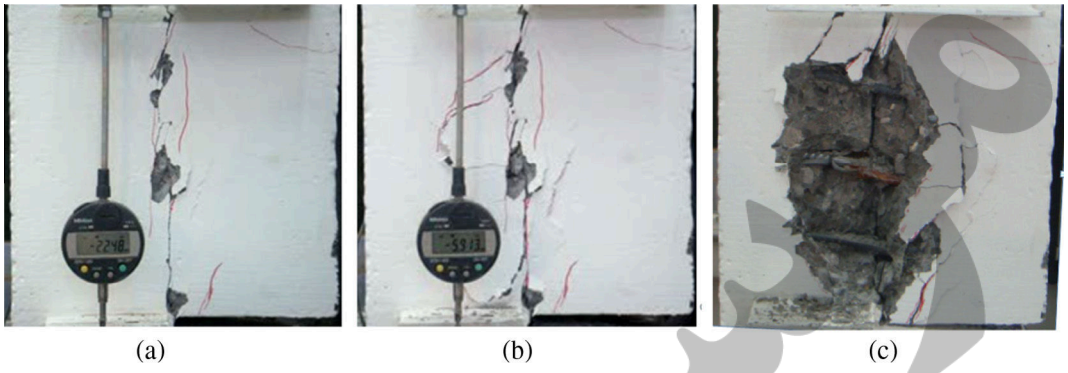


**Fig. 5.** Conditions of specimen 70-3T8-SCC. (a) Right after ultimate stress, (b) at slip of about 6 mm, and (c) after final release of load.

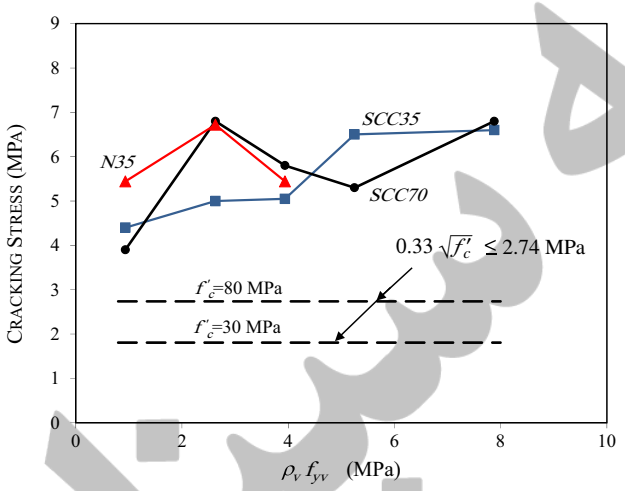


**Fig. 6.** Cracking shearing stresses versus amount of clamping reinforcement.

compressive strength had a limited effect on the cracking stresses of the SCC specimens. Increasing $f_{cu}$ from 43.7 MPa to 79.2 MPa caused an average increase in $v_{cr}$ of less than 5%. It is to be noted that the size of the maximum aggregate was smaller in the high strength concrete series of specimens. However, this is not likely to be the cause of the limited difference in $v_{cr}$ in the two SCC series. The effect of the aggregate size on the cracking strength of pushoff specimens has not been experimentally studied. However, in beam shear, the aggregate size has an effect the ultimate shear resistance, but not as much on the first cracking shear stress. The aggregate size is included in the calculation of the concrete resistance (e.g. Ref. [2]) when these equations are based on the ultimate strength of longitudinally reinforced beams and not on their first cracking stress [25]. The ultimate strength includes a significant contribution from aggregate interlock, which is effectively activated after the occurrence of cracking [26].

A commonly used equation for the cracking in members subjected to predominant shear is that of the ACI code [1] and is given by:

$$v_{cr\text{-}A} = 0.33\sqrt{f'_c} \leq 2.74\,\text{MPa} \quad (1)$$

The upper limit in Eq. (1) reflects the fact that the increase in cracking shearing strength is limited in HSC. The calculations of Eq. (1) corresponding to 30 MPa and 80 MPa concrete are plotted in Fig. 6. The comparison shows that the results of Eq. (1) are very conservative for the estimation of the cracking stresses in pushoff type specimens.

Fig. 6 shows that increasing $\rho_v f_{yv}$ caused a slight increase in $v_{cr}$, but this increase was very limited for levels larger than 5.25 MPa. On the other hand, Table 1 did not show a significant effect of the amount of longitudinal reinforcement on the cracking stresses, as the difference in $v_{cr}$ remained within the natural scatter of the results. However, these observations are based on a limited number of tests and hence they need to be carefully interpreted.

### 3.3. Yield stresses

Fig. 7 shows the shear stress versus the tensile strain in the clamping bars in the specimens of the SCC35 series. A sharp softening is observed in the response curves before the observation of surface cracking. This softening is an indication of the occurrence of cracking. It is typically accompanied by a change in the mechanism of resistance, where the reinforcement is more efficiently engaged in the clamping the shear-transfer plane due to the occurrence of crack separation [19,26]. A similar behavior is observed in conventional beam shear tests [27]. Fig. 7 also suggests that the internal cracking has developed before the surface cracking could be visually detected.

The values of $v_y$ and of the ratios ($v_y/v_u$) are shown in Table 1. The fifteen ratios ranged from 0.74 to 1.0, and their average and coefficient of variation were 0.92% and 8.2%, respectively. This is in line with the common assumption in shear-friction models (e.g. [1–3]) that the clamping steel yields at ultimate conditions. However, shear-friction models are generally based on the test results of precracked specimens and cold-joint specimens. The results reported in this work confirm that this assumption is also valid for non-precracked specimens.

### 3.4. Ultimate and residual strength

Table 1 gives the ratios of the residual strength $v_r$ to the ultimate strength $v_u$. The fifteen ratios ranged from 0.23 to 0.74, and their average and coefficient of variation were 0.44 and 28.2%, respectively.

Fig. 8 plots the ultimate strength $v_u$ and the post-ultimate strength $v_r$ versus the amount of clamping steel ($\rho_v f_{yv}$). For the SCC specimens of the same series which contained similar amounts of clamps, average values are plotted.

The figure shows that in general, larger levels of clamping reinforcement increased the ultimate strength. It also shows a similar effect on the residual strength for reinforcement ratios $\rho_v f_{yv}$ up about 4 MPa. At larger amounts of ($\rho_v f_{yv}$), the residual strength was limited to maximum values between 5 and 6 MPa. It is to be noted that the shear-friction model in the ACI code [1] limits the nominal strength to 5.5 MPa for shear transfer across cold joints which have not been intentionally roughened.

The normal strength SCC specimens (SCC35) and the conventional concrete specimens (N35) had nearly equal concrete cube

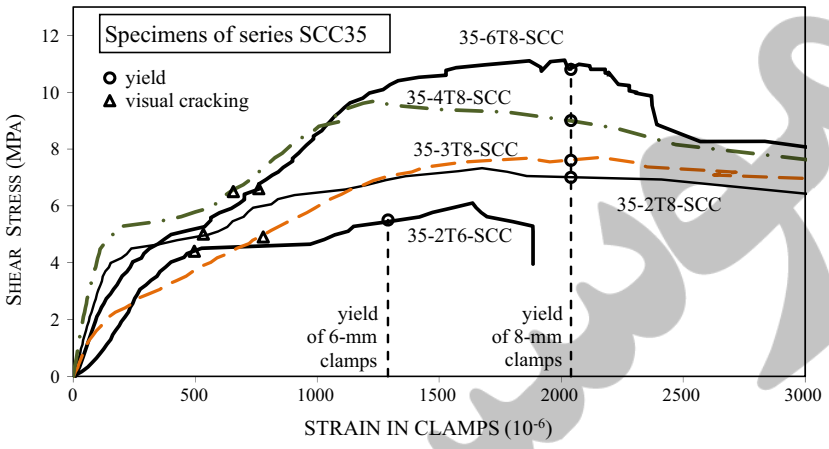


**Fig. 7.** Strains in the clamps of specimens of series SCC35.

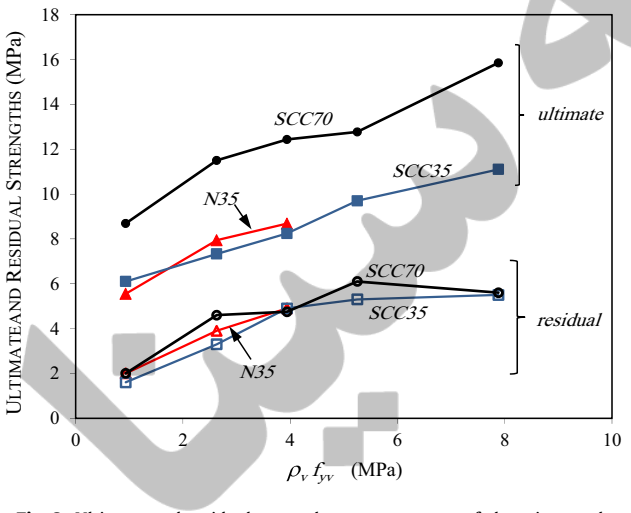


**Fig. 8.** Ultimate and residual strengths versus amount of clamping steel.

strength. The size of the maximum aggregate was the same in both mixes, but the gradation was different. Table 1 and Fig. 8 show that their ultimate strength and residual strength showed similar trends. The difference in ultimate strengths ranged from 8% to 11% and in residual strengths from 14% to 20%. The SCC specimen with the smallest ($\rho_v f_{yv}$) was stronger than the corresponding specimen of series N35, but the two N35 specimens with larger clamping steel were stronger than the corresponding SCC35 specimens. An opposite trend is observed when comparing the residual strengths. With the limited number of tests, limited difference in ultimate strengths and the normal variation observed in shear test results, more tests are required to accurately establish the effect of using concrete with self-compacting properties on the pushoff strength of normal strength concrete.

Fig. 8 also shows that the specimens of the high-strength concrete series (SCC70) resisted significantly larger ultimate shearing stresses than the specimens of series SCC35. This indicates that the concrete strength has a considerable effect on the ultimate strength of SCC. However, Fig. 8 also shows that the concrete strength had a limited effect on the residual strength. It is noted that the size of the maximum aggregate in series SCC70 and SCC35 was 10 mm and 20 mm, respectively. A larger aggregate size is likely to provide a larger resistance by aggregate interlock [26,27] once cracking is initiated. However, a stronger concrete resists more efficiently degradation when subjected to complex stresses due to dowel action [28] and bearing and shearing stresses from the aggregate interlock [29].

At ultimate conditions, the high strength concrete specimens had superior dowel action and concrete matrix, which exceeded the advantage provided by the larger aggregate size in the normal strength concrete. This led to a significantly larger ultimate shear resistance in the HSC specimens.

In the post-ultimate range, the difference in the dowel action resistance between the HSC and the NSC specimens is significantly reduced because of the severe spalling of the side cover. The fracture and plastification of the core concrete across the interface is generally severe [28], especially in the concrete with smaller size aggregates. The reductions in the aggregate interlock and dowel action were more significant in the HSC specimens, and did offset the advantages provided by the HSC. This is in line with the trends observed in Fig. 8 where limited difference was observed between the residual strength of NSC and HSC.

The specimens which contained different longitudinal (vertical) reinforcement resisted different yield, ultimate and residual strengths. The average difference for the two series was less than 8% for the yield strength and for the ultimate strength, and about 17% for the residual strength. Differences in the order of 10–15% are not uncommon in shear tests. For example, the ultimate shearing strength of two duplicate specimens in series 1 of the landmark tests conducted by Hofbeck et al. [7] differed by as much as 10%. In addition, it is likely that the presence of additional vertical bars in the vicinity of the shear transfer plane, and the fact that they were discontinued in this region, created further disturbance along the critical plane and affected the strength results.

## 4. Comparison with analytical results

The experimentally observed ultimate strengths are compared with the calculations of four models: the ACI shear-friction model [1], the AASHTO modified shear friction model [2], Mattock's modified shear-friction model [3] and Rahal's simplified SMCS model [23]. These models are applicable to the case where the critical transfer planes were not pre-cracked. In addition, the experimentally observed residual strengths are compared with the calculations of four models: the ACI [1], AASHTO [2] and Mattock's models, and the EC2 code [24]. The following presents the basic equations of these models for the case where the concrete on either sides of the interface is normal-density, the clamping steel is perpendicular to the critical shear-transfer plane, and no additional forces are applied perpendicular to the direction of the

transfer plane. Resistance and material reduction factors are taken as unity.

### 4.1. ACI shear-friction model

The ACI [1] nominal strength is given by:

$$v_{ACI} = \mu\rho_v f_{yv} \leqslant \begin{bmatrix} 0.2f'_c \\ 3.3 + 0.08f'_c \\ 11\ \text{MPa} \end{bmatrix} \quad (2)$$

The term $\mu$ is a coefficient to account for friction. It is taken as 1.4 for concrete cast monolithically, 1.0 for concrete cast against hardened concrete whose surface is intentionally roughened, and 0.6 if the surface is not intentionally roughened. It is appropriate to use $\mu = 1.4$ for the calculation of the ultimate strength of non-precracked specimens presented in this study. The upper limits given in Eq. (2) are suitable for monolithic construction and for the case where the concrete is cast against hardened concrete whose surface is intentionally roughened. For surfaces that are not intentionally roughened, the upper limits are $0.2f'_c$ and 5.5 MPa.

### 4.2. AASHTO modified shear-friction model

The AASHTO LRFD [2] nominal strength is given by:

$$v_{AASHTO} = c + \mu\rho_v f_{yv} \leqslant \begin{bmatrix} 0.25f'_c \\ 10.3\ \text{MPa} \end{bmatrix} \quad (3)$$

where the terms ($c$) and ($\mu$) are taken as 2.8 MPa and 1.4 for monolithic construction, and 1.7 MPa and 1.0 for concrete cast against hardened concrete whose surface is intentionally roughened, respectively. For surfaces that are not intentionally roughened, the two terms are taken as 0.52 MPa and 0.6, respectively, and the upper limits are changed to $0.2f'_c$ and 5.5 MPa.

### 4.3. Mattock's model

For monolithic construction and across the interface when concrete is placed against hardened concrete with its surface intentionally roughened, the nominal strength calculated using Mattock's modified shear-friction model [3] is given by:

$$v_{Mat} = \begin{bmatrix} 2.25\rho_v f_{yv} & \text{when} \quad \rho_v f_{yv} \leqslant K_1/1.45 \\ K_1 + 0.8\rho_v f_{yv} & \text{when} \quad \rho_v f_{yv} > K_1/1.45 \end{bmatrix} \quad (4a)$$

but not greater than ($0.3f'_c$) nor 16.5 MPa. The factor $K_1$ is taken as ($0.1f'_c$) but not greater than 5.5 MPa for monolithic construction, and as 2.8 MPa for the intentionally roughened surfaces.

For concrete placed against hardened concrete not intentionally roughened, the strength is similar to that of the ACI code for the same conditions:

$$v_{MAT} = 0.6\rho_v f_{yv} \leqslant \begin{bmatrix} 0.2f'_c \\ 5.5\ \text{MPa} \end{bmatrix} \quad (4b)$$

### 4.4. SMCS model

The nominal strength calculated using the simplified model for combined stress-resultants (SMCS) [23,29,30] is given by the following equation:

$$v_{SMCS}/f'_c = \sqrt{\omega_L \times \omega_v} \leqslant \kappa \quad (5)$$

where the reinforcement indexes are calculated as $\omega_L = \rho_L f_{yL}/f'_c \leqslant \kappa$ and $\omega_v = \rho_v f_{yv}/f'_c \leqslant \kappa$ and the upper limit $\kappa$ is taken as $(1/3 - f'_c/900)$. In pushoff specimens, the term $\omega_L$ is taken as the upper limit ($\kappa$) [23].

### 4.5. Eurocode 2

The EC2 [24] provisions are applicable to shear transfer across the interface of concretes cast at different time. The general equation for the strength is given by:

$$v_{EC2} = cf_{ctd} + \mu\rho_v f_{yv} \leqslant 0.5\eta f_{cd} \quad (6)$$

where $\eta$ is a strength reduction factor given by $0.6(1 - f_{ck}/250)$, and $f_{ctd}$, $f_{cd}$ and $f_{ck}$ are the design tensile strength, design compressive strength, and characteristic compressive strength of concrete, respectively. The coefficients $c$ and $\mu$ are taken as 0.5 and 0.9 for surfaces with indentations, 0.45 and 0.7 for rough surfaces such as those achieved by raking, and 0.35 and 0.6 for smooth surfaces left without treatment after vibrations, respectively.

### 4.6. Observed versus calculated ultimate strengths

The ACI, AASHTO, Mattock and SMCS models are applicable to the case of monolithic construction, where the critical transfer planes were not pre-cracked. They are used to calculate the ultimate strength of all the specimens. The EC2 equations are valid for the case of concretes cast at different times and hence are not directly applicable for calculating the ultimate strength of non-precracked concrete. Table 4 summarizes the calculations of the four models and lists the ratios between the observed and calculated strengths.

Fig. 9(a) compares the observed ultimate strength for series SCC35 against the calculations of the four models described earlier. The residual strength is also shown for comparison. Since the specimens were not precracked, the friction factor μ is taken as 1.4 in Eqs. (2) and (3). Fig. 9(b) shows a similar comparison for series SCC70.

It is shown that nearly all calculated strengths are conservative. The best correlation average was achieved by AASHTO's model, but the least coefficient of variation was achieved by the SMCS model, as also expected from Fig. 9(a) and (b). The ACI code results are significantly more conservative than the remaining ones.

## 5. Calculations of residual strength

Mattock et al. [14] and Kahn and Mitchell [4] observed that after reaching the ultimate shear strength, non-precracked pushoff specimens resisted a residual strength which was similar to the strength of the precracked specimens. Rahal and Al-Khaleefi [16] concluded that precracking reduces the ultimate strength to a value between the non-precracked strength and the residual strength, depending on the severity of the precracking.

Precracking is commonly achieved by placing the specimen horizontally on the test machine and applying vertical line loads on the opposite faces of the shear transfer plane until the formation of the crack along the plane. While the use of this method is very common, the extent of the cracking it causes is not. In many cases (e.g. [4,7]) the crack widths and the steel strains are not reported. When reported, a large variation in the crack widths due to precracking is observed. For example, the precracking of the large-scale specimens tested by Nagle and Kuchma [11] led to crack widths ranging from 0.03 to 0.86 mm. It is expected that precracking to larger crack widths leads to ultimate shearing strengths closer to the residual strength.

The loading of non-precracked elements to ultimate strength causes considerable cracking in addition to yielding of the clamping bars. See Fig. 4. These conditions are considered similar to

**Table 4**
Comparison between experimental and calculated ultimate strengths.

| Specimen | $v_u$ (MPa) | $v_{u\text{-}ACI}$ (MPa) | $v_{u\text{-}AASHTO}$ (MPa) | $v_{u\text{-}MAT}$ (MPa) | $v_{u\text{-}SMCS}$ (MPa) | $\frac{v_u}{v_{u\text{-}ACI}}$ | $\frac{v_u}{v_{u\text{-}AASHTO}}$ | $\frac{v_u}{v_{u\text{-}MAT}}$ | $\frac{v_u}{v_{u\text{-}SMCS}}$ |
|---|---|---|---|---|---|---|---|---|---|
| 35-2T6-SCC | 6.10 | 1.31 | 4.11 | 2.10 | 3.10 | 4.67 | 1.49 | 2.90 | 1.97 |
| 35-2T8-SCC | 7.33 | 3.68 | 6.48 | 5.60 | 5.20 | 1.99 | 1.13 | 1.31 | 1.41 |
| 35-3T8-SCC | 7.70 | 5.52 | 8.32 | 6.65 | 6.37 | 1.40 | 0.93 | 1.16 | 1.21 |
| 35-3T8-SCCr | 8.79 | 5.52 | 8.32 | 6.65 | 6.37 | 1.59 | 1.06 | 1.32 | 1.38 |
| 35-4T8-SCC | 9.70 | 6.10 | 8.74 | 7.70 | 7.35 | 1.59 | 1.11 | 1.26 | 1.32 |
| 35-6T8-SCC | 11.1 | 6.10 | 8.74 | 9.80 | 9.01 | 1.82 | 1.27 | 1.13 | 1.23 |
| 70-2T6-SCC | 8.69 | 1.31 | 4.11 | 2.10 | 4.29 | 6.65 | 2.12 | 4.14 | 2.02 |
| 70-2T8-SCC | 11.50 | 3.68 | 6.48 | 5.92 | 7.21 | 3.12 | 1.77 | 1.94 | 1.60 |
| 70–3T8-SCC | 12.57 | 5.52 | 8.32 | 8.65 | 8.82 | 2.28 | 1.51 | 1.45 | 1.43 |
| 70-3T8-SCCr | 12.3 | 5.52 | 8.32 | 8.65 | 8.82 | 2.23 | 1.48 | 1.42 | 1.39 |
| 70-4T8-SCC | 12.77 | 7.35 | 10.15 | 9.70 | 10.2 | 1.74 | 1.26 | 1.32 | 1.25 |
| 70-6T8-SCC | 15.85 | 9.80 | 10.30 | 11.8 | 12.5 | 1.62 | 1.54 | 1.34 | 1.27 |
| 35-2T 6-0 | 5.55 | 1.31 | 4.11 | 2.10 | 3.35 | 4.24 | 1.35 | 2.64 | 1.66 |
| 35-2T 8-0 | 7.94 | 3.68 | 6.48 | 5.92 | 5.62 | 2.16 | 1.22 | 1.34 | 1.41 |
| 35-3T 8-0 | 8.68 | 5.52 | 8.32 | 7.33 | 6.87 | 1.57 | 1.04 | 1.18 | 1.26 |
| | | | | Average | | 2.58 | 1.35 | 1.72 | 1.45 |
| | | | | C.O.V. (%) | | 58.0 | 23.0 | 49.6 | 17.4 |

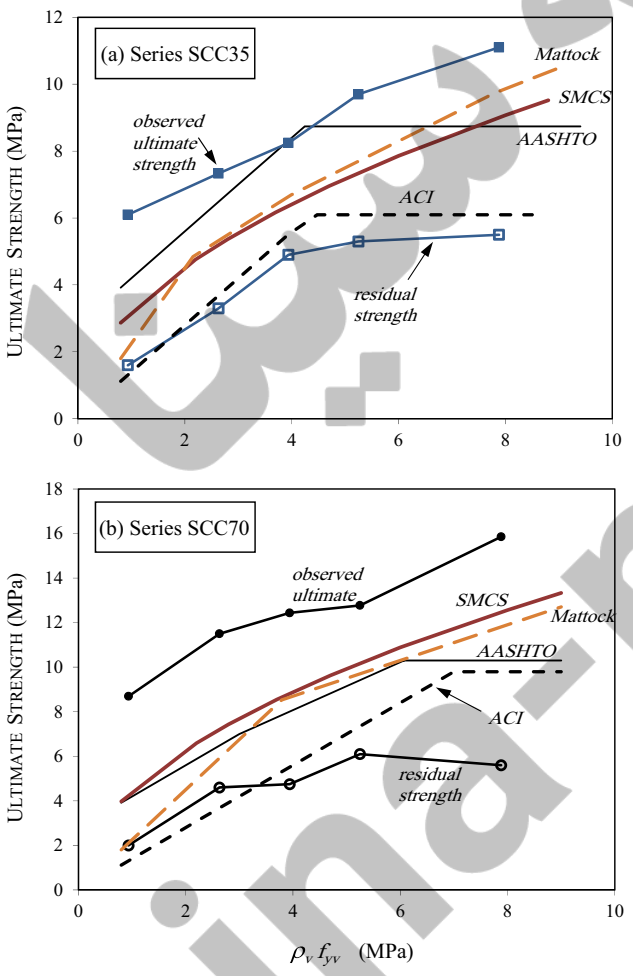


**Fig. 9.** Experimental versus calculated ultimate strengths of specimens from SCC series.

severe precracking, which render the strength to be equal to the residual strength. Consequently, it is suggested that the residual strength can be calculated using the strength equations relevant to precracked elements.

This strength of precracked elements depends considerably on the roughness of the surface [1–3]. It has been observed that shearing cracks in normal strength concrete pass through the cement paste and around the aggregates, leading to significant aggregate interlock. However, the cracks in high strength concrete pass through both the paste and the aggregates leading to smoother cracks [27,31]. To account for this observation, it has been suggested that the value of the maximum size of aggregates that is used in calculating the concrete contribution in concrete of strength higher than 70 MPa to be taken as zero [32]. Consequently, a relatively rough surface can be expected along the shear transfer planes of NSC specimens, while a smoother surface can be expected for the HSC specimens.

Table 5 compares the experimentally observed residual strength with the calculations of four methods: ACI, AASHTO, EC2 and Mattock's. The ACI, AASHTO and Mattock calculations for series SCC35 and N35 are based on the equations for intentionally roughened surfaces while those for series SCC70 are based on the equations for surfaces not intentionally roughened (closer to smooth surfaces). The EC2 calculations are based on the equations for rough surfaces for series SCC35 and N35, and for smooth surfaces for series SCC70.

Fig. 10 compares the observed residuals strengths with the calculated values for the SCC series. For the sake of comparison, the figure includes the calculations of each of the methods based on the two surface roughness conditions discussed earlier. Table 5 and Fig. 10 show that the ACI equations provide generally conservative results. The upper limits for intentionally roughened surface conditions are slightly unconservative, and the more restrictive limits of the smoother surface conditions are more suitable. In addition, the use of $\mu = 0.6$ for the SCC70 series is very conservative, and a value of 1.0 is more appropriate. The results of AASHTO and of Mattock's model for intentionally roughened surface conditions severely over-estimate the strength of the normal strength series, while the model for surfaces without intentional roughening is considerably conservative for the high strength series. The use of a cohesion factor was one of the main reasons for the unconservative results of AASHTO and Mattock's methods. A cohesion coefficient $c$ equal to zero is reasonable because pushoff specimens without clamping steel fail after reaching ultimate and do not possess any residual strength [16]. The EC2 provides the best correlation with the experimental results as shown in Table 5. However, it is shown in Fig. 10 that the upper limits can be significantly unconservative.

Fig. 11 shows a plot of the residual strength versus the clamping stress for all the specimens reported in this paper in addition to those from 15 specimens reported elsewhere [16]. The cube

**Table 5**
Comparison between experimental and calculated residual strengths.

| Specimen | $v_r$ (MPa) | $v_{r\text{-}ACI}$ (MPa) | $v_{r\text{-}AASHTO}$ (MPa) | $v_{r\text{-}EC2}$ (MPa) | $v_{r\text{-}MAT}$ (MPa) | $\frac{v_r}{v_{r\text{-}ACI}}$ | $\frac{v_r}{v_{r\text{-}AASHTO}}$ | $\frac{v_r}{v_{r\text{-}EC2}}$ | $\frac{v_r}{v_{r\text{-}MAT}}$ |
|---|---|---|---|---|---|---|---|---|---|
| 35-2T6-SCC | 1.6 | 0.93 | 2.63 | 1.50 | 2.10 | 1.71 | 0.61 | 1.06 | 0.76 |
| 35-2T8-SCC | 3.3 | 2.63 | 4.33 | 2.69 | 5.60 | 1.25 | 0.76 | 1.23 | 0.59 |
| 35-3T8-SCC | 5.6 | 3.94 | 5.64 | 3.61 | 6.65 | 1.42 | 0.99 | 1.55 | 0.84 |
| 35-3T8-SCCr | 4.2 | 3.94 | 5.64 | 3.61 | 6.65 | 1.07 | 0.74 | 1.16 | 0.63 |
| 35-4T8-SCC | 5.3 | 5.25 | 6.95 | 4.52 | 7.70 | 1.01 | 0.76 | 1.17 | 0.69 |
| 35-6T8-SCC | 5.5 | 6.10 | 8.74 | 6.37 | 9.80 | 0.90 | 0.63 | 0.86 | 0.56 |
| 70-2T6-SCC | 2.0 | 0.56 | 1.08 | 1.71 | 0.56 | 3.57 | 1.85 | 1.17 | 3.57 |
| 70-2T8-SCC | 4.6 | 1.58 | 2.10 | 2.73 | 1.58 | 2.92 | 2.19 | 1.69 | 2.92 |
| 70-3T8-SCC | 4.6 | 2.36 | 2.88 | 3.51 | 2.36 | 1.95 | 1.60 | 1.31 | 1.95 |
| 70-3T8-SCCr | 4.9 | 2.36 | 2.88 | 3.51 | 2.36 | 2.07 | 1.70 | 1.40 | 2.07 |
| 70-4T8-SCC | 6.1 | 3.15 | 3.67 | 4.30 | 3.15 | 1.94 | 1.66 | 1.42 | 1.94 |
| 70-6T8-SCC | 5.6 | 4.73 | 5.25 | 5.88 | 4.73 | 1.18 | 1.07 | 0.95 | 1.18 |
| 35-2T 6-0 | 2.0 | 0.93 | 2.63 | 1.64 | 2.10 | 2.14 | 0.76 | 1.22 | 0.95 |
| 35-2T 8–0 | 3.9 | 2.63 | 4.33 | 2.83 | 5.92 | 1.48 | 0.90 | 1.38 | 0.66 |
| 35-3T 8-0 | 4.9 | 3.94 | 5.64 | 3.75 | 7.33 | 1.24 | 0.87 | 1.31 | 0.67 |
| | | | | Average | | 1.72 | 1.14 | 1.26 | 1.33 |
| | | | | C.O.V. (%) | | 43.1 | 45.1 | 17.1 | 70.9 |

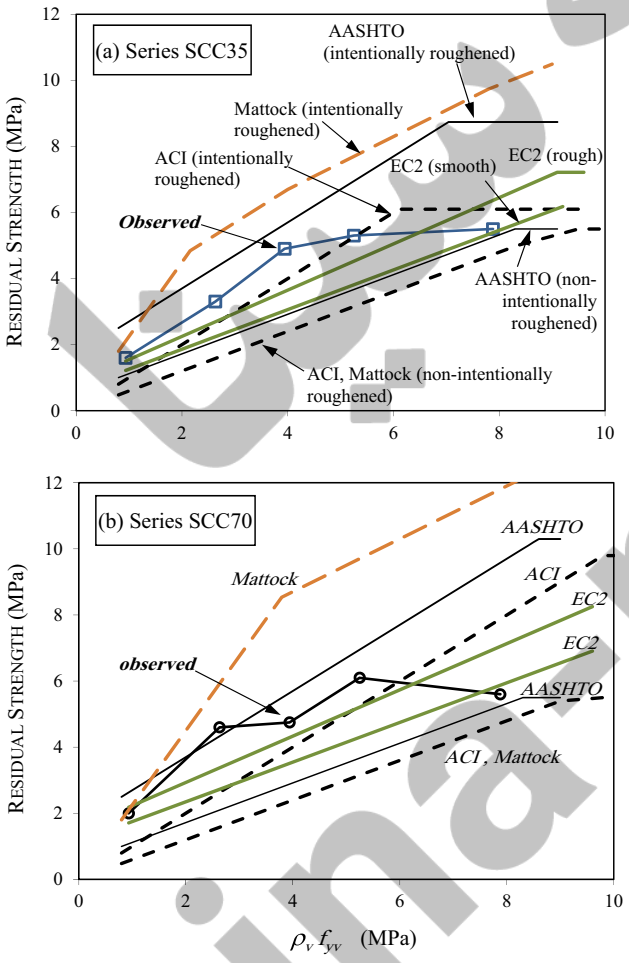


**Fig. 10.** Experimental versus calculated residual strengths of specimens from SCC series.

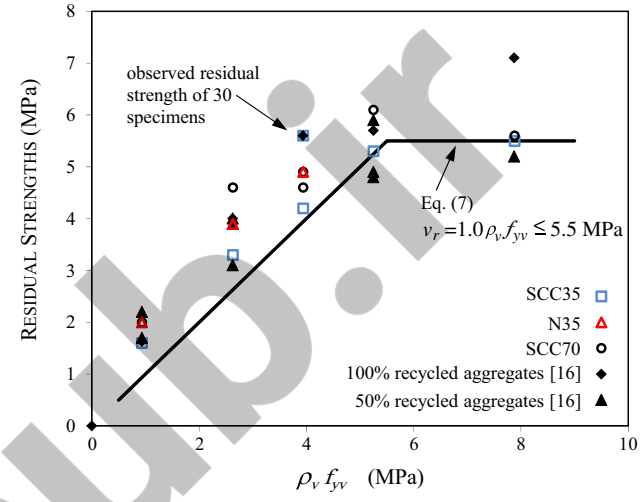


**Fig. 11.** Residual strengths versus clamping reinforcement.

compressive strength of these specimens ranged from 29.3 to 54.7 MPa, and the concrete was made by replacing 50% or 100% of the coarse aggregates with recycled ones. One of the specimens did not contain clamping bars. It failed when cracking was first observed and did not possess any residual strength. Fig. 11 shows that the residual strength increases with larger clamping. The maximum stress that can be relied on is between 5 and 6 MPa. Based on the test results in Fig. 11, it is suggested that the residual strength can be calculated using the following equation which satisfies the restriction of $c = 0$:

$$v_r = 1.0\rho_v f_{yv} \leqslant 5.5 \text{ MPa} \quad (7)$$

Eq. (7) is plotted in Fig. 11 and is shown to be adequate for the calculation of the residual strength of all 30 specimens.

## 6. Conclusions

Tests were conducted on 15 non-precracked pushoff specimens to study the shear behavior of normal strength and high-strength SCC. The following are the main conclusions of the study:

1. Increasing the compressive strength of the concrete led to a significant increase in the ultimate shearing strength of the push-off specimens. However, it had a limited effect on the cracking stresses and on the post-ultimate residual stresses.
2. Increasing the amount of clamping reinforcement increased the ultimate strength. It also increased the residual strength but was limited to an upper value of 5–6 MPa in specimens with relatively large clamping steel

3. The ultimate strength was typically reached when the strains in the clamping steel reached the yield values. The ratio of the yield to the ultimate strengths ranged from 0.75 to 1.0, with an average of 0.93 and a coefficient of variation of 8.2%.
4. The ultimate strengths were compared with the calculations of four models, including the ACI and the AASHTO shear-friction models. The calculated strengths were generally conservative. The best correlation average was obtained using AASHTO's model, but the best coefficient of variation was obtained using the SMCS model.
5. The possibility of using four existing models to calculate the residual strength was investigated, assuming that the conditions of the transfer planes in NSC and HSC specimens are similar to those of surfaces which are intentionally roughened and surfaces which are not intentionally roughened, respectively. It was found that the results of EC2 provided the best correlation with the experimental results, while those of the ACI code provided generally conservative results.
6. It is suggested that a using the shear friction general equation with a coefficient of cohesion $c = 0$, a coefficient of friction $\mu = 1.0$, and an upper limit on the stress equal to 5.5 MPa provides adequate calculation of the residual strength in pushoff specimens which were not pre-cracked.
7. The ACI equation for web shear cracking provides a very conservative estimate of the stresses at cracking in the concrete.

## Acknowledgment

This research was made possible by a Grant from Research Sector at Kuwait University, Kuwait, Grant No. EV03/08. This support is gratefully acknowledged.

## References

[1] ACI committee 318. Building code requirements for structural concrete (ACI 318-11) and commentary (ACI 318R-11). American Concrete Institute; 2011.
[2] AASHTO LRFD bridge design specifications. American Association of State Highway and Transportation Officials, 4th ed., SI units ed.; 2007 [1526p].
[3] Mattock AH. Shear-friction and high-strength concrete. Am Concr Inst Struct J 2001;98(5):50–9.
[4] Kahn LF, Mitchell AD. Shear friction tests with high-strength concrete. ACI Struct J 2002;99(1):98–103.
[5] Walraven J, Frénay J, Pruijssers A. Influence of concrete strength and load history on the shear friction capacity of concrete members. PCI J 1987;32(1):66–84.
[6] Mattock AH, Johal L, Chow HC. Shear transfer in reinforced concrete with moment or tension acting across the shear plane. PCI J 1975;20(4):76–93.
[7] Hofbeck JA, Ibrahim IO, Mattock AH. Shear transfer in reinforced concrete. J Am Concr Inst 1969;66(2):119–28.
[8] Júlio ENBS, Dias-da-Costa D, Branco FAB, Alfaiate JMV. Accuracy of design code expressions for estimating longitudinal shear strength of strengthening concrete overlays. Eng Struct 2010;32:2387–93.
[9] Incea R, Yalcina E, Arslanb A. Size-dependent response of dowel action in R.C. members. Eng Struct 2007;29:955–61.
[10] Xiao J, Xie H, Yang Z. Shear transfer across a crack in recycled aggregate concrete. Cem Concr Res 2012;42:700–9.
[11] Nagle TJ, Kuchma DA. Shear transfer resistance in high-strength concrete girders. Mag Concr Res 2007;59(8):611–20.
[12] Walraven JC, Stroband J. Shear friction in high-strength concrete, high-performance concrete. Am Concr Inst SP-149 1994:311–30.
[13] Mattock AH. Shear transfer under monotonic loading across an interface between concretes cast at different times. Univ. of Washington report SM 76-3; 1976 [66 pp].
[14] Mattock AH, Li WK, Wang TC. Shear transfer in lightweight reinforced concrete. PCI J 1976;21(1):20–39.
[15] Anderson AR. Composite designs in precast and cast-in-place concrete. Progr Architect 1960;41(9):172–9.
[16] Rahal KN, Al-Khaleefi AL. Shear-friction behavior of recycled and natural aggregate concrete. ACI Struct J 2015;112(6):725–33.
[17] Sagaseta J, Vollum RL. Influence of aggregate fracture on shear transfer through cracks in reinforced concrete. Mag Conc Res 2011;63(2):119–37.
[18] Shaw DM. Direct shear transfer of lightweight aggregate concretes with non-monolithic interface conditions. MSc thesis. Missouri University of Science and Technology; 2013 [141 pp].
[19] Harries KA, Zeno G, Shahrooz B. Toward an improved understanding of shear-friction behavior. ACI Struct J 2012;109(6):835–44.
[20] Haskett M, Oehlers DJ, Ali MSM, Sharma SK. Evaluating the shear-friction resistance across sliding planes in concrete. Eng Struct 2011;33:1357–64.
[21] Santos PMD, Júlio ENBS. A state-of-the-art review on shear-friction. Eng Struct 2012;45:435–48.
[22] Xu J, Wu C, Li ZXi, Ng CT. Numerical analysis of shear transfer across an initially uncrack reinforced concrete member. Eng Struct 2015;102:296–309.
[23] Rahal KN. Shear-transfer strength of reinforced concrete. ACI Struct J 2010;107(4):419–26.
[24] EN 1992-1-1. Eurocode 2: design of concrete structures—Part 1-1: general rules and rules for buildings. European Committee for Standardization, Brussels, Belgium; 2004.
[25] Rahal KN, Collins MP. Background of the 1994 CSA-A23.3 general method of shear design. Can J Civ Eng 1999;26(6):827–39.
[26] Walraven JC. Aggregate interlock: a theoretical and experimental analysis. Diss. TU Delft, Delft University of Technology; 1980.
[27] Collins MP, Mitchell D. Prestressed concrete structures. Englewood Cliffs, N. J.: Prentice-Hall Inc.; 1991.
[28] Maekawa K, Qureshi J. Shear transfer across interfaces in reinforced concrete due to aggregate interlock and dowel action. JSCE 1997;34(557):159–72.
[29] Rahal KN. Simplified design and capacity calculations of shear strength in reinforced concrete membrane elements. Eng Struct 2008;30:2782–91.
[30] Rahal KN. Post-cracking shear modulus of reinforced concrete membrane elements. Eng Struct 2010;32:218–25.
[31] Cladera A, Mari AR. Experimental study on high-strength concrete beams failing in shear. Eng Struct 2005;27:1519–27.
[32] CSA-A23.3. Design of concrete structures (A23.3-04). Canadian Standards Association, Canada; 2004 (reapproved 2010) [214 p].